Effect of Moving Ice Loads on the Plastic Capacity of a Ship's Structure

Bruce W.T. Quinton
Memorial University of Newfoundland
St. John's, Newfoundland, Canada
Bruce.Quinton@nrc-cnrc.gc.ca
Claude G. Daley
Memorial University of Newfoundland
St. John's, Newfoundland, Canada
cdaley@mun.ca
Robert E. Gagnon
National Research Council of Canada – Institute for Ocean Technology (NRC-IOT)
St. John's, Newfoundland, Canada
Robert.Gagnon@nrc-cnrc.gc.ca

ABSTRACT

The IACS unified polar rules define the design ice load as a glancing impact on the bow shoulder. The load and structural response model in the polar rules ignore the tangential motions and assumes the interaction occurs at one location. If the impact duration were sufficient, the ice may "score" along the hull during a glancing impact. This paper examines the questions of how structure responds to moving loads, in comparison to normal loads. An explicit nonlinear numerical model was created and validated against full-scale physical experiments. Moving load scenarios were then simulated. The structure's capacity to withstand moving loads causing "progressive damage" was found to be generally less than its capacity to withstand static loads.

KEY WORDS: moving load; ice scoring; progressive damage; progressive plastic damage; glacial ice load.

INTRODUCTION

The IACS polar rules design scenario is a glancing impact of the ship's bow with an ice edge (IACS 2007). Further, this glancing load is applied statically to the ship's structure. This design scenario does not address the possible effects of the ice "scoring" the ship's hull during the impact. Scoring due to ice may be described as a moving ice load that causes damage as it progresses along the hull (i.e. progressive damage) leaving an elongated "dent" in its wake. It is therefore of interest to determine the reaction of a ship's structure to moving ice loads. Some motivating questions include: *Are the assumptions associated with a static structural analysis valid when a moving load causes progressive damage? Does progressive damage affect the structures resistance to further damage? What are the structural failure mechanisms associated with progressive damage from moving ice loads?*

Investigation of structural phenomena associated with moving ice loads causing progressive damage was carried out using an explicit nonlinear numerical model. This model was based on – and validated against – full-scale experiments involving large steel grillages that were designed to check the IACS polar class structural limit state formulations. After validation, eight progressive damage scenarios were imposed on the numerical model. These eight load scenarios were chosen to explore the response of the grillage to various types of scoring ice loads.

Progressive Damage

Progressive damage can be viewed as plastic structural damage due to the scoring action of ice as it moves along the hull. Progressive damage occurs when the relative tangential movement of ship and ice is large enough to extend the damage laterally during the collision. This type of interaction can happen at the waterline or below. Waterline damage may result from collision with pack ice, glacial ice of various size (from growler to iceberg), or level-ice during ice-channel navigation (assisted or unassisted). Damage below the waterline may occur from a deep collision with glacial ice, the keel of a pressure ridge, a deep impact from a single ice fragment forced under the hull or from contact with ice trapped between a vessel and the sea bottom.

Progressive damage is similar to the "raking" damage observed during grounding incidents, however the tearing and subsequent curling of the hull steel (Zhang, 2002) was not treated because ice-strengthened ships are expected to survive such impacts without tearing of the hull plating (within their operational capacity).

Load Scenarios

The eight progressive damage scenarios investigated may be divided into three categories: progressive damage between two stringers, progressive damage spanning two stringers and progressive damage parallel to the stringers. Five levels of indentation were simulated for each scenario; for a total of 40 progressive damage load cases.

While progressive damage scenarios are inherently dynamic (i.e. they are largely affected by phenomena that depend on time), these eight progressive damage scenarios were modeled without material strain-rate effects, velocity dependent friction and rigid body ship motions. Omitting these time-dependent effects removed the dependence of the structural response on the velocity of the moving load; thereby reducing the number of variables in the analyses.

LARGE GRILLAGE PHYSICAL EXPERIMENTS

The numerical model used for this research was based on – and validated against – the large grillage experiments discussed in this section.

These physical experiments involved statically loading a full-scale IACS classed ship's grillage well into the realm of plastic response. They were designed and carried out by Daley and Hermanski (2008a; 2008b). They are the most recent in a series of experiments that are part of a comprehensive study of the ultimate strength of ships' frames. These studies were jointly funded by Transport Canada, the United States Coast Guard, and the US-Canada Ship Structures Committee.

Large Grillage Model

The large grillage model (top of Figure 1) is a full-scale representation of the side shell of a PC6 IACS ice-strengthened ship (IACS 2007). It is a 6.756 m long by 1.5 m wide stiffened plate structure with a plate thickness of 10 mm. The stiffening is provided by two 325 x 18 / 120 x 18 FF stringers at a spacing of 2000 mm, and three 200 x 8 / 75 x 10 FF transverse stiffeners at a frame spacing of 350 mm. The model was constructed entirely of 350MPa steel.

The steel at the boundaries of the large grillage structure does not correspond directly to any part of an ice-strengthened ship's structure; instead, it was designed to provide boundary conditions for the stiffened plate structure consistent with the boundary conditions that would exist if the model was infinitely surrounded by identical grillage structure (Daley and Hermanski 2008b).

Boundary Conditions

During the experiments, the large grillage model was fixed to a robust steel test frame (the large grillage is shown mounted to the test frame in the lower part of Figure 1).

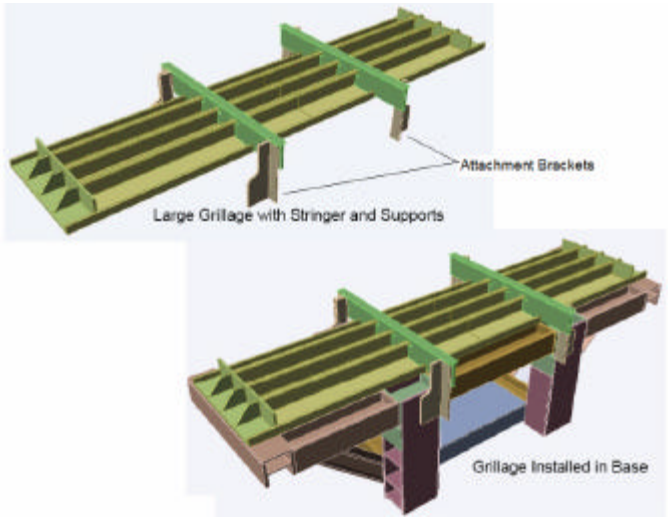

Figure 1. Large grillage model – isometric view.

It was expected that no plastic deformation of the test frame took place during the experiments, and because the plastic deformations of the large grillage model were so large, any elastic deformation of the test frame is considered negligible.

The large grillage structure was bolted to the test frame at its longitudinal ends (see Figure 2), and at ends of the stringers using the attachment brackets shown in Figure 1. The bolt patterns at all attachment points were such that motion was restrained in all six degrees of freedom (DOF).

Figure 2. Large grillage end boundary condition.

Loading Scenario

The load was applied to large grillage model as a small patch, normal to the shell plating. Loads were applied between the two stringers at locations along the central transverse stiffener. A 500 kip hydraulic ram was used to apply the load through a 130 mm x 130 mm steel block (henceforth called the indenter). To "soften" stress concentrations that would otherwise arise in the presence of sharp edges, a thin spacer plate was placed between the block and the shell plating. This spacer plate folded over the sharp edges of the steel block and prevented the block from cutting into the shell.

NUMERICAL MODEL

An explicit nonlinear finite element code was required in order to model progressive damage scenarios. Progressive damage involves large structural deformations which require nonlinear geometric and nonlinear material modeling capabilities. Collision and scoring are also intrinsic phenomena of progressive damage that require explicit time integration and contact detection.

MPP-DYNA is an explicit nonlinear finite element code that exhibits these required capabilities. It is a release of the proven and popular LS-DYNA code that is capable of running in parallel on multiple computers in a cluster. MPP-DYNA was used exclusively throughout this research.

The numerical model was created at full scale, and was based on the full-scale IACS polar class large grillage experiments described above.

Geometry and Mesh

The large grillage numerical model was composed entirely of planar areas (see Figure 3) including everything shown in the top of Figure 1; except the "attachment brackets". These areas were meshed with

standard 4-node shell elements with five through thickness integration points. The Belytschko-Tsay element formulation was used for all shell elements. This element formulation includes bending, membrane and shell thickness changes. It also employs reduced integration, includes transverse shear and has built in hourglass control. Reduced integration is desirable because it increases the speed of finite element calculations and it alleviates *shear locking*; which is a phenomenon common with 4-node (i.e. lower order) shell element meshes.

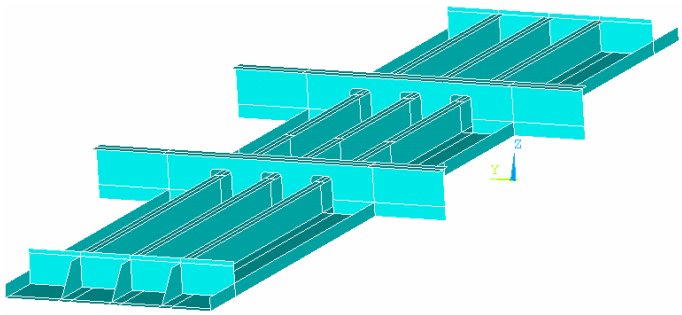

Figure 3. Numerical model large grillage geometry.

The indenter (i.e. the 130 mm x 130 mm steel block placed between the hydraulic ram and the plate during the physical experiments) was modeled using standard 8-node brick (i.e. solid) elements. Solid elements were used because the indenter is not thin compared with its length and width.

The indenter used in the large grillage experiments was of sufficient size and thickness that it was not expected to suffer any plastic deformation. The magnitude of the plastic damage to the large grillage structure is very large compared to the indenter's elastic deformation; therefore, this elastic deformation is considered negligible. For this reason the indenter was modeled as a rigid body.

A mesh convergence study was conducted and the results converged for a mesh density of 4279 elements/m^2; resulting in a total number of shell elements of 80,874 (mesh shown in Figure 4).

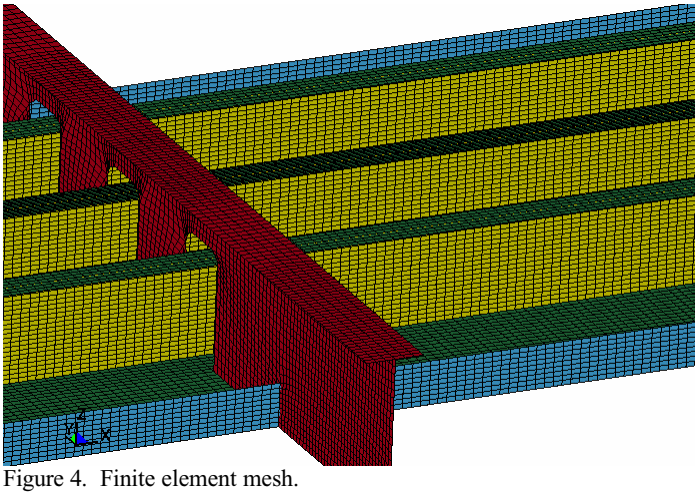

Figure 4. Finite element mesh.

Material Models

Two material models were employed: a bilinear isotropic elasto-plastic model for the large grillage and a rigid model for the indenter.

Physical material tensile tests were carried out on steel from the various components of the physical large grillage structure. Paik's "knock-down factor approach" (Paik, 2007) was used to resolve the bilinear material model inputs from the engineering stress-strain results of the tensile tests. The same bilinear isotropic elasto-plastic model was applied throughout the entire large grillage numerical model; with the following inputs:

Table 1. Large Grillage material model parameters.

Density [kg/m^3]	Young's Modulus [Pa]	Poisson's Ratio	Yield Stress [Pa]	Tangent Modulus [Pa]
7850	2.00E+11	0.3	3.50E+08	1.00E+09

The rigid material model was applied to the indenter; with identical inputs as in Table 1 (as required).

Boundary Conditions

The bolt patterns used to attach the large grillage structure to the test frame during the physical experiments were such that rotations and displacements in all degrees of freedom were fixed. Nodes in the numerical model that were coincident with the location of these bolts were constrained in all rotational and translational DOF.

Contact

Loads were applied to the large grillage structure by imposing controlled displacements on the rigid indenter. Implementation of a contact algorithm in these simulations was necessary to allow the indenter to interact with the large grillage model. A surface-to-surface contact algorithm was employed. Shell element thickness was accounted for during contact.

Damping

Tests of the numerical model during its development revealed that structural oscillations were evident in the 120-150 Hz range. These oscillations were the "ringing" in the large grillage structure post initial contact with the indenter. This "ringing" was damped out by applying 20% critical damping to the entire structure over the 120-150 Hz range. The choice of 20% critical damping was the result of a sensitivity study on the effect of damping on the numerical model results.

NOTES ON LOADING, ANALYSIS AND RESULTS OF THE NUMERICAL MODEL

Loading Method

Progressive damage causes nonlinear stress-strain behaviour; therefore, the method of load application is important because the principle of superposition does not hold. The method of load application used for this investigation consists of three separate actions: first, the indenter is pushed into the hull plating (z-direction motion only); next, the indenter is dragged laterally (x- and/or y-directions only); and third, the indenter is pulled out of the hull plating (again in the z-direction only). Henceforth, the first loading action will be referred to as the *static load*, the second will be referred to as the *moving load*, and the third action will be referred to as *unloading*.

This loading method was chosen because it is the simplest method with which to study progressive damage. Each change in the indenter's motion is independent, enabling observation of its effects on the structure. Examples of two load-history curves resulting from the application of this loading method are given in Figure 5.

It was generally observed that the structural capacity of the large grillage model was lower for a large *moving load* than for an equivalent *static load*. The initial part of a curve (denoted by a green "S" in the figure) shows the resultant structural reaction to the *static load*. The second part of a curve (denoted by a red "D" in the figure) shows the resultant structural reaction to the *moving load*. The third part of a curve shows the structural reaction during *unloading*. For brevity, the *unloading* section is not denoted; but it follows the other two sections.

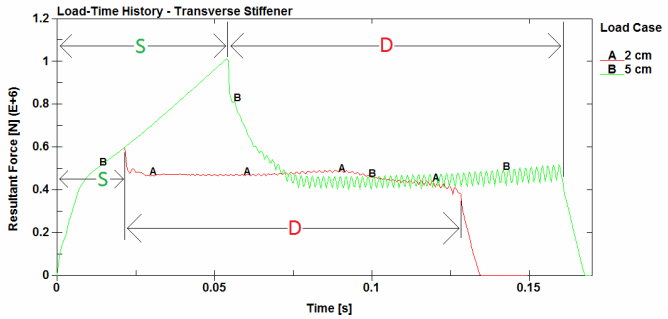

Figure 5. Example load-time history curves for two load cases – for each case the *static load* portion (i.e. z-force reaction only) is denoted by the green "S" and *moving load* portion is denoted by the (red "D").

The final value of the *static load* part of a curve is the large grillage's *static structural capacity*; which is also the reaction force at the start location of the *moving load*. This value represents the structure's reaction to a simple z-direction indentation at this lateral location (i.e. (x,y)) on the grillage. Any value along the *moving load* part of a curve may be referred to as the *moving load structural capacity*. This value represents the structure's reaction to a moving z-direction indentation that has caused previous damage at other locations throughout the structure.

Each progressive damage scenario was designed such that the *moving load* stops at a lateral location that is symmetrically opposite from that of its start location. Further, the large grillage structure is itself a symmetric structure. Because both the structure and the start and finish locations of the *moving load* are symmetric, a direct comparison between the static structural capacity and the moving load structural capacity may be made for these locations. Further, static indentations for various other lateral locations were carried out. These other locations were chosen to be in the path of the *moving loads* for the various progressive damage scenarios. Knowledge of the static structural reactions at these locations enabled further comparison between the structure's static and moving load structural capacities.

Note that the indenter's velocity during the *static load* and the *unloading* was the same for all load cases; as was the indenter's lateral velocity (although lateral velocity was not equal to z-velocity). The family of load curves presented in Figure 5 have *moving* sections that all take the same length of time, indicating that the lateral distance travelled by the indenter was the same for each. The *static* sections all take different amounts of time, indicating that the level of indentation into the plate was different for each case.

Eight progressive damage load scenarios were considered. These eight load scenarios may be broken into three categories: progressive damage between stringers, progressive damage across multiple stringers, and progressive damage parallel to stringers. Table 2 illustrates the categories and scenarios examined.

For each load scenario, five load cases were tested. The length of the *dynamic load* (i.e. scoring length) was the same for each load case, but the *static loads* (i.e. indentation depths) were not. These *static loads* were equal to 0.1%L, 0.25%L, 1%L, 2.5%L, and 5%L; where L is the stringer spacing of the large grillage. This spacing is L=2000 mm; therefore the applied *static loads* were: 0.2, 0.5, 2.0, 5.0, and 10.0 cm indentations. Each load case is referred to in this paper by its *static load* indentation value. Given that there are eight load scenarios with five load cases per scenario, 40 progressive damage tests were performed.

Table 2: Progressive damage design scenarios investigated.

Category	Scenario
Between Stringers	Between Transverses
	Along Transverses
	Diagonally Across Transverses
Across Stringers	Between Transverses
	Along Transverses
	Diagonally Across Transverses
Perpendicular to Stringers	Between Transverses
	Along Transverses

Material failure was not modeled in these simulations, and therefore the finite elements could strain to infinity. For this reason the results for the 10 cm load cases (and sometimes the 5 cm load cases, as outlined where necessary) should not be viewed as predicting the actual behaviour or structural capacity of the structure. In all likelihood, the large grillage structure would rupture under these extreme load conditions. The 10 cm load cases were performed in order to obtain an exaggerated view of the phenomena occurring during lower load cases.

Notes on Plots of Results

The results of each test are given in the form of load-displacement plots, and various other figures. Unless otherwise stated, all load-displacement curves report the structures resultant reaction force versus the lateral displacement of the indenter. That is, the total force pushing on the indenter compared to the indenters motion in the plane of the hull plating. Note that these "load versus lateral displacement" curves show that the reaction force does not start from zero at zero displacement. This is valid because the *static load* (i.e. z-direction indentation) has already occurred before any lateral indenter motion takes place; therefore, there is already a large z-force on the indenter when the lateral motion is still zero, and hence a large resultant force at the start of the load-displacement curves. Note that the resultant force for the *static load* is always in the z-direction (i.e. normal to the plate). Resultant force vectors for the *static* and *moving loads* are illustrated in Figure 6.

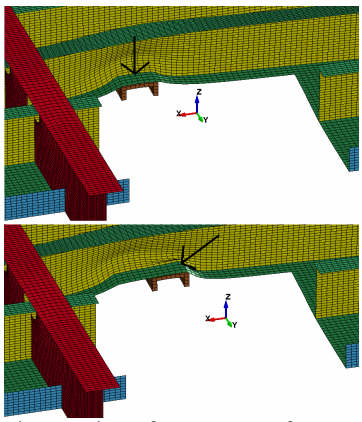

Figure 6. Illustrative resultant force vectors for *static load* (top) and *moving load* (bottom).

RESULTS

The results of the progressive damage load scenarios investigated show a general decrease in the capacity of the "IACS polar class" large grillage structure to carry large *moving loads*, versus large *static loads*. The level of decrease in structural capacity was found to depend on the depth of indentation into the structure, the location of the progressive damage and the extent of the progressive damage. The structural mechanisms associated with this decrease were found to arise at the transition from a *static* to a *moving load* (i.e. the transition from initial impact to scoring). *Static loads* were shown to induce a symmetric structural response throughout the structure adjacent to the load (where symmetry was permitted by the geometry of the structure). This symmetrical response was retained for *moving loads* that induced a grossly elastic structural response; but upon commencement of *moving loads* causing progressive damage, this symmetry vanished. The magnitude of the associated bending moments, membrane stresses, and through-thickness shear reactions were all generally smaller on the trailing side of a large *moving load* than on the leading side. Further, previous plastic damage to large structural members (such as the stringers) was shown to have a definite weakening effect on the structural capacity of the structure adjacent to them.

For brevity, only significant results from the 40 load cases are presented here. The reader is referred to Quinton (2008) for the results of each load case.

Symmetric Structural Response – Static and Grossly Elastic Moving Loads

Static loads always induced a symmetric structural response (where permitted by the geometry of the structure); that is, all structure radially adjacent to the point of application of a *static load* participated relatively equally in response to that load. This response symmetry is evident in Figure 7; which shows various type of structural reactions to a 2 cm static indentation (i.e. *static load*).

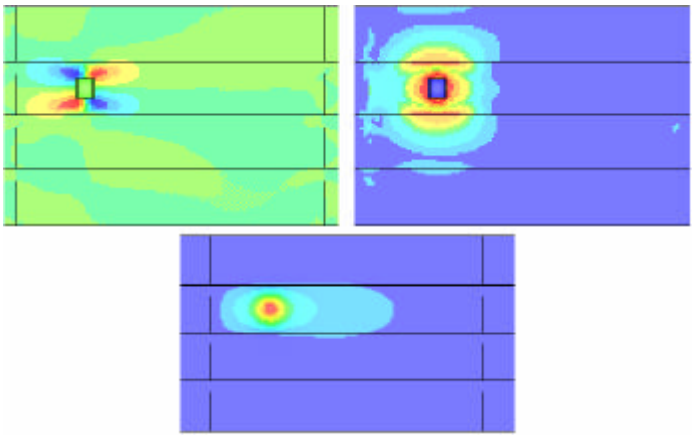

Figure 7. Results for a 2 cm static indentation between stringers and transverse stiffeners. Top left – *Mxy* moment distribution; top right – maximum in plane stress; bottom – z-displacement (i.e. depth of the "dent"). Note: the indenter is also shown in the top two plots.

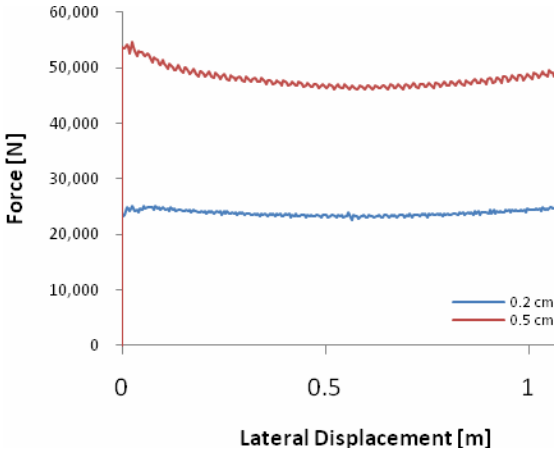

Figure 8 shows the structure's resultant reaction force versus lateral (i.e. dragged) displacement for *moving loads* of 0.2 and 0.5 cm indentation that were imposed on the hull plating between two stringers and between two transverse stiffeners. As mentioned above, the start and finish locations of the *moving loads* were symmetric about the centre of the structure; and structure itself is symmetric about its lateral (i.e. *x*-*y*) axes. This implies that the loads at the start and finish of the *moving load* should be equal. Indeed, this is true for the 0.2 cm load case. This case (shown as line *A* in

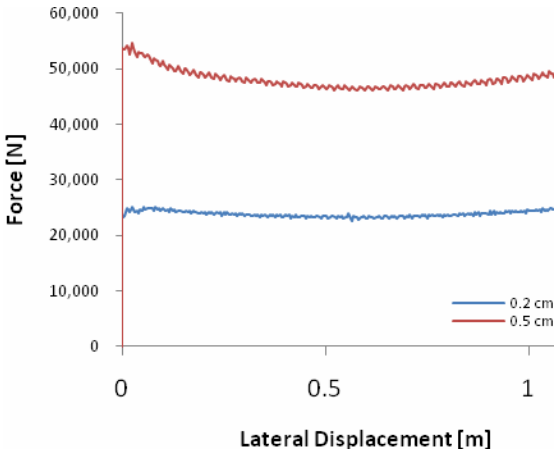

Figure 8) exhibits a symmetric "bowl-shaped" reaction curve; that is, the start and finish loads (i.e. at zero lateral displacement and maximum lateral displacement, respectively) are equal; as are all other loads symmetric about the centerline of the large grillage. The minimum and maximum lateral displacements plotted correspond to positions on the grillage close to the stringers, while the central lateral displacement corresponds to the position directly between the stringers. The response at the centre of the large grillage is lower than near the stringers because the structure is less stiff at this location. The plastic damage associated with this 0.2 cm load case was negligible.

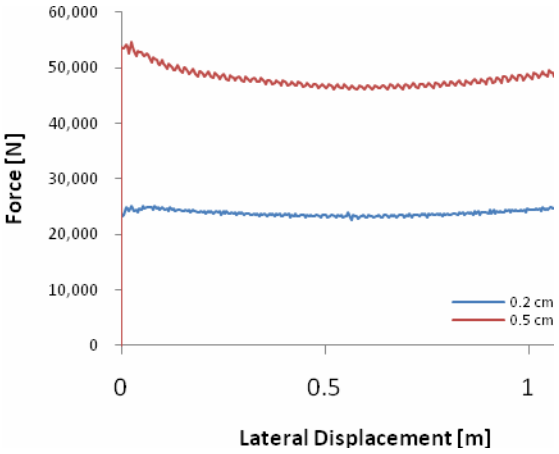

Figure 8. Reaction force versus lateral load displacement for 0.2 and 0.5 cm (indentation) *moving loads* between stringers and transverses.

Elastic/plastic Transition Response

The 0.5 cm load case exhibits a similar "bowl shaped" reaction curve as to the 0.2 cm case, but does not exhibit the same symmetry about the centerline of the large grillage; specifically, its initial load is higher than its final load. If the structure was loaded *statically* at both locations, these reactions would be identical due to the symmetry of the structure. The fact that they are not equal in

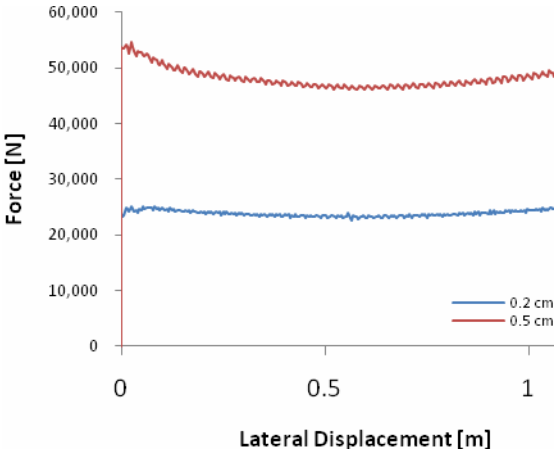

Figure 8 indicates that the progressive nature of the load affected the overall response of the structure. These unequal responses result from prior plastic damage done to the structure as the load advanced to its final position. The fact that the overall shape of the load-deflection curve is relatively smooth indicates that the progressive damage is yet small, and the gross elastic response of the undamaged surrounding structure is still important.

Asymmetric Structural Response – Moving Loads causing Progressive Damage

Further to the 0.2 and 0.5 cm load cases shown in Figure 8, Figure 9 shows structural reaction curves for the 2, 5 and 10 cm load cases. For high indentation loads, a distinct and immediate drop in structural capacity is observed upon commencement of the *moving load*. The initial plastic damage was much greater for these load cases than for the 0.2 and 0.5 cm load cases. This large amount of initial plastic damage caused an asymmetric structural reaction as the load began to move. Analysis of these load cases has shown that – because the structure on the trailing side of the *moving load* was plastically damaged – its ability to exert a reaction force on the indenter via bending and through-thickness shear was compromised; and the reaction force was provided primarily by the undeformed structure on the leading side of the *moving load.*

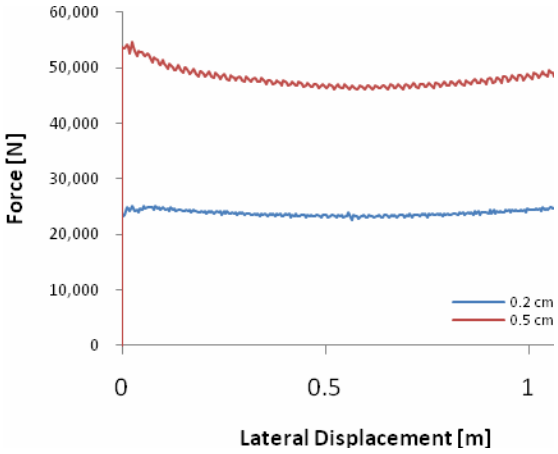

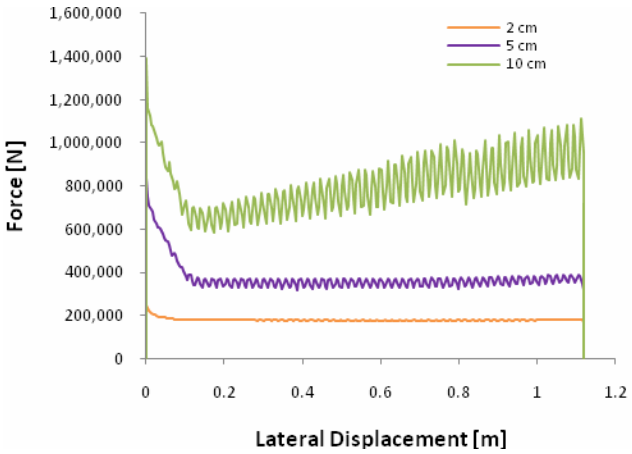

Figure 9. Reaction force versus lateral load displacement for 2, 5, and 10 cm (indentation) *moving loads* between stringers and transverses.

Figure 10 shows plots of through thickness shear, *Q*, for the 2 cm load case. The top two sections of this figure show *Qx* (left) and *Qy* (right) for the *static load*; where the symmetrical structural reaction discussed above is evident. The lower two sections show *Qx* (left) and *Qy* (right) after commencement of the *moving load*; where the lack of a symmetric structural reaction is also evident. Notice that in the lower plots, the through thickness shear on the leading edge of the indenter remains relatively unchanged, while on the trailing side of the indenter it has been severely compromised.

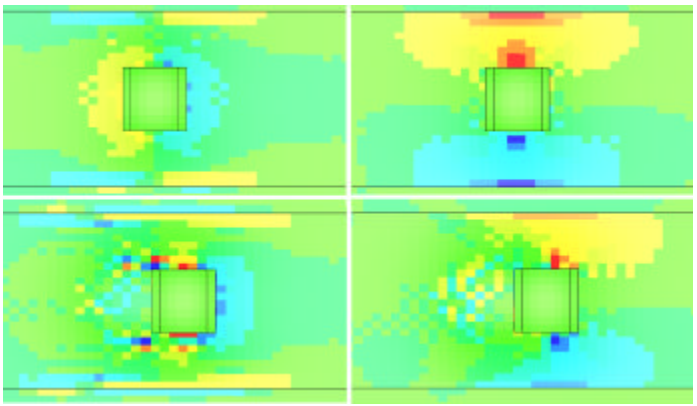

Figure 10. Plots of *Qx* (left) and *Qy* (right) for the 2cm load case between stringers and transverses (indenter shown). The top plot for each shows the *static load* structural reaction while the bottom plot shows the subsequent *moving load* reaction.

Figure 11 shows the *Mxy* bending moment distribution for two snapshots of the *moving load* for the 2 cm load case. Note: the *static load Mxy* plot for this load case is given in Figure 7. It can be seen from this plot that the *Mxy* symmetry about the indenter shown in Figure 7 is no longer evident and that – similar to the through thickness shear reaction – it has been compromised on the trailing side of the *moving load.*

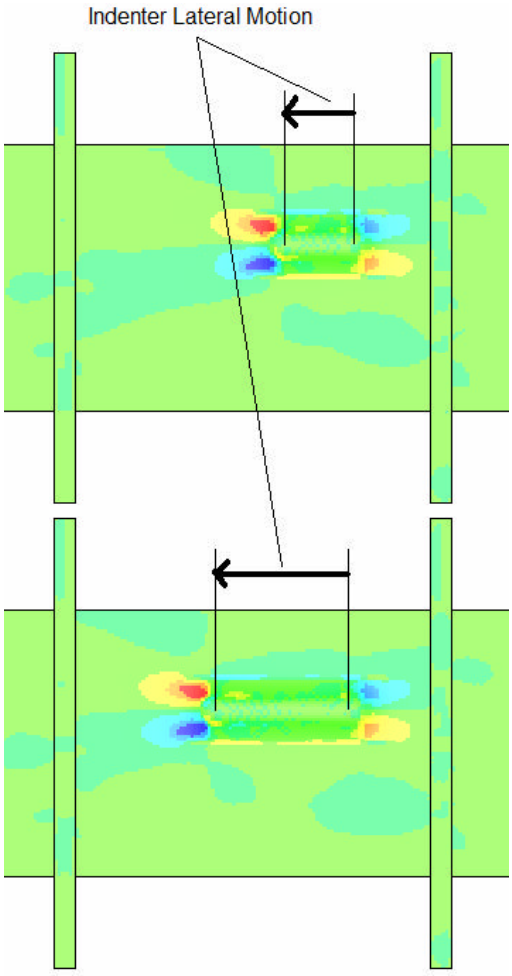

Figure 11. *Mxy* moment distribution for the 2cm load case (between stringers and transverses) during the *moving load* portion (indenter not shown).

Moving Loads crossing Stringers

Figure 12 presents the results of a scenario where *moving loads* were applied along a transverse stiffener that crossed two stringers. The results of the numerical model were not valid for the 5 and 10 cm load cases and hence are left out of this figure. The humps in the curves correspond to the encounters between the indenter and the stringers. Similar to the scenario discussed above, the 0.2 and 0.5 cm load cases for this scenario show a relatively elastic gross structural reaction and exhibit "bowl-shaped" response curves between the stringers. Also as above, the large (2 cm) load case shows an initial decrease in capacity upon commencement of the *moving load*; however a new unique structural behavior associated with *moving loads* was evident. In addition to the decrease in bending and through-thickness shear capacity outlined previously, stiffener buckling was observed at a much lower level of indentation for *moving loads* than for *static loads*. Specifically, while transverse stiffener buckling was observed for the *moving load* at an indentation of 2 cm (see Figure 13), it was not observed in the same location for a *static load* until an indentation of at least 7 cm was achieved.

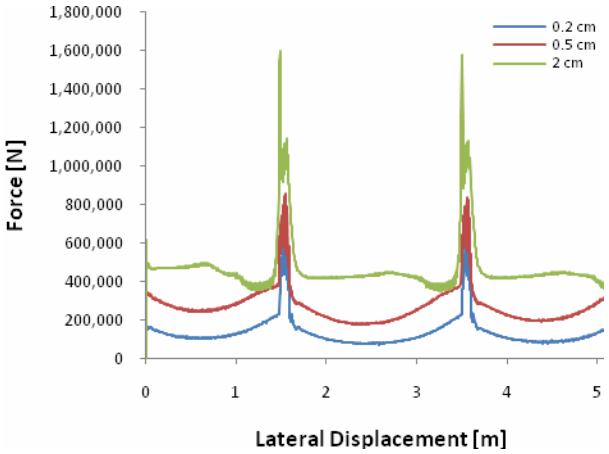

Figure 12. Reaction force versus lateral load displacement for 0.2, 0.5 and 2 cm (indentation) *moving loads* along a transverse and across stringers.

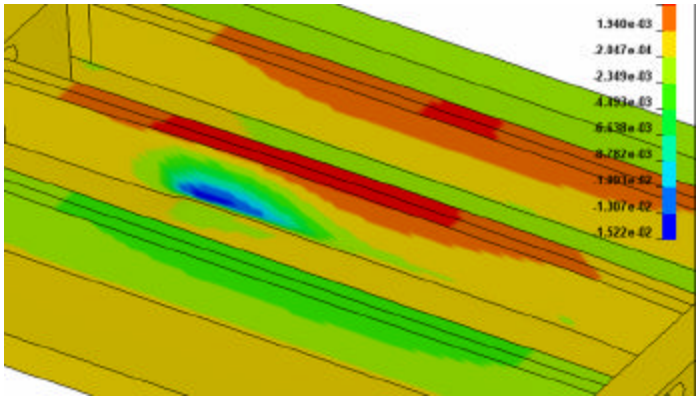

Figure 13. Central transverse stiffener buckling for a 2 cm *moving load* case.

It was mentioned above that previous plastic damage to large structural

members (such as the stringers) was shown to have a definite weakening effect on the capacity of the structure adjacent to them. This is evident in the 0.2 and 0.5 cm load cases presented in Figure 12; that is, if one examines the resultant reaction force as the indenter approaches a stringer and compares it with the reaction force immediately after the stringer has been damaged, it is evident that the reaction force of the structure is significantly lower post stringer damage. This behavior is not evident for the 2 cm load case because of the onset of transverse stiffener buckling as the indenter approaches a stringer.

CONCLUSIONS AND RECOMMENDATIONS

These results, though preliminary, illustrate the need to consider the effects of moving ice loads on the structural response of ice-classed ship structures. It appears that moving loads may cause significantly more structural damage than purely normal loads. It is evident from this research that these loads cannot be treated with traditional static design methods. These effects will require further consideration as plastic design is increasingly employed.

ACKNOWLEDGEMENTS

The numerical modeling work for this research was carried out at the Institute for Ocean Technology - National Research Council of Canada on their Beowulf cluster; with much gratitude.

REFERENCES

IACS, "Requirements Concerning Polar Class", International Association of Classification Societies (IACS), London, 2007.

Daley, C. G., and Hermanski G., "Ship Frame Research Program - An Experimental Study of Ship Frames and Grillages Subjected to Patch Loads, Volume 1 - Data Report", Ship Structure Committee, SSC Project SR 1442 - Final Report; OERC Report 2008-001; NRC-IOT Report TR-2008-11, 2008a.

Daley, C. G., and Hermanski G., "Ship Frame Research Program - An Experimental Study of Ship Frames and Grillages Subjected to Patch Loads, Volume 2 - Theory and Analysis Reports", Ship Structure Committee, SSC Project SR 1442 - Final Report; OERC Report 2008-001; NRC-IOT Report TR-2008-11, 2008b.

Paik, J. K., "Practical Techniques for Finite Element Modeling to Simulate Structural Crashworthiness in Ship Collisions and Grounding (Part I: Theory)", *Ship and Offshore Structures* Vol. 2, Issue 1, 2007.

Quinton, B. (2008). "*Progressive Damage to a Ship's Structure due to Ice Loading*", M. Eng. Thesis, Memorial University of Newfoundland

Zhang, S., "Plate tearing and bottom damage in ship grounding", *Marine Structures* vol.15 Issue 2, March, 2002.